저압 화학 기상 증착법을 이용한 실리콘 표면 위의
텅스텐 박막의 증착

金 聖 薰

서울대학교 자연과학대학 화학과

(1993. 8. 27 접수)

Deposition of Tungsten Thin Film on Silicon Surface by
Low Pressure Chemical Vapor Deposition Method

Sung Hoon Kim

Department of Chemistry, Seoul National University,
Seoul 151-742, Korea

(Received August 27, 1993)

요 약. 저압 화학 기상 증착법을 사용하여 WF_6의 환원반응으로 텅스텐 박막을 p형 실리콘 (100) 표면 위에 증착하였다. Cold-wall 조건에서는 실리콘 기판과 SiH_4를 각각 이용하여 WF_6를 환원시켜 텅스텐 박막을 증착하였으며 hot-wall 조건에서는 WF_6를 SiH_4로 환원시켜 증착하였다. 박막의 결정구조는 어느 조건에서나 체심입방구조를 이루었으며, 증착조건에 따른 박막의 물리적 및 전기적 특성을 조사하였다. 증착된 박막을 온도 800℃에서 열처리한 결과 hot-wall 조건의 박막이 WSi_2로 변화하였다. 실험적 결과들과 이론적인 고찰들로부터 열처리에 따른 박막의 결정구조와 특성 변화의 원인을 규명하였다. Hot-wall과 cold-wall 조건에서의 박막을 분석한 결과 박막의 특성은 cold-wall 조건이 우수하나 hot-wall 조건에서는 열처리 방법에 의하여 실리콘 기판과 적합성이 우수한 것으로 알려진 WSi_2 박막의 제조가 가능함을 알 수 있었다.

ABSTRACT. Tungsten thin film was deposited on p-(100) silicon substrate by using the LPCVD(low pressure chemical vapor deposition) technique. WF_6 was used as a source gas for tungsten and SiH_4 was used as a reducing gas for WF_6. Tungsten thin film was deposited by either SiH_4 or Si substrate reduction of WF_6 under cold-wall condition and it was deposited by SiH_4 reduction of WF_6 under hot-wall condition. The crystal structure of deposited thin film under both conditions were identified to be bcc (body centered cubic). The physical and electrical properties of deposited thin films were investigated. The deposited film under hot-wall condition changed to WSi_2 film by the annealing under 800℃. From the experimental results and theoretical considerations, the change of the crystal structure of the thin film by annealing was discussed. WSi_2 thin film, which was known to have good compatibility with Si substrate, could be produced under hot-wall condition although the film properties were superior under cold-wall condition.

INTRODUCTION

Electrical resistivity in interconnect lines and contact resistance increase as the VLSI system develops to the more complicated level in which minute size and high quality are required in semiconductor devices. In spite of the small device size, the source voltage constant, so the high power electrical density causes electromigration of interconnect lines and contact parts[1]. In aluminum, a soft material, the migration of atoms induced by such electromigration effects can produce "holes" in thin film, sometimes even leading to disconnection

金 聖 蕉

of the interconnect line[2,3]. Thus low electrical resistivity as well as hardness are required for new materials to replace aluminum. Refractory metals, such as tungsten and molybdenum, and their silicides, such as WSi_2 and $MoSi_2$ have been regarded as good candidates to replace aluminum[4,5]. Among these materials, tungsten is of particular interest because it has a similar thermal expansion coefficient with silicon[6]. Moreover, it is known to have deposition selectivity, that is, it is deposited only on silicon surface[7]. So it has the cutoff advantage of the masking step in semiconductor processes.

There are many well-known thin film deposition techniques for use in semiconductor processes that include vacuum evaporation, ion sputtering, and chemical vapor deposition[7]. Among these techniques, LPCVD (low pressure chemical vapor deposition) method has many advantages and has been widely used in semiconductor processes[8,9]. LPCVD method utilizes the reaction between gas reactants and solid surface, which eventually leads to the formation of thin films on solid substrate. In tungsten LPCVD WF_6 is usually used as a tungsten source gas[10] for its usefulness, while, SiH_4, with the advantage of compatibility with silicon substrate, and H_2 are used as reducing gases[11,12].

In this work, in order to obtain the desired low electrical resistivity and good compatibility, we used SiH_4 as a reducing gas and deposited tungsten thin film on silicon substrate with or without using reducing gas in LPCVD system. The physical and electrical properties were investigated and discussed. The deposition reaction was carried out using both hot-wall reactors to determine the effect of reactor design. The fundamental deposition mechanism and the effect of annealing were also discussed.

EXPERIMENTAL

The LPCVD system of cold-wall type is shown in *Fig.* 1. The reactor wall was water-cooled. The hot-wall reactor was made by setting 17 cm(W)× 17 cm(L)×26 cm(H) of stainless steel shroud around the heater. The temperature of the resistance heater was uniformly controlled during the
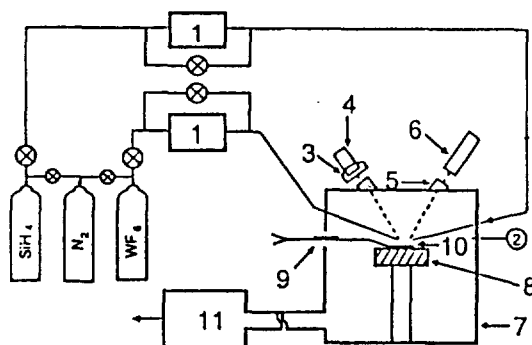

Fig. 1. Schematic diagram of LPCVD system. 1: Mass flow controller, 2: Pressure gauge, 3: Monochromator, 4: Photo diode, 5: Sapphire window, 6: He-Ne Laser, 7: Reactor, 8: Heater, 9: Thermocouple, 10: Substrate (Si wafer), 11: Pump.

Table 1. Experimental conditions in LPCVD reactions

Case	Flow rate (sccm)	Reaction temp. (°C)	Pressure (mTorr)	Reaction time (min.)
WF_6 only	WF_6 (36)	450	150	30
$WF_6 + SiH_4$	WF_6 (36) SiH_4 (18)	450	250	30

reaction using the front side K type thermocouple (Chromel-Alumel) and a temperature controller (Omega 4001KC). WF_6 (99.99%, Takachiho) and SiH_4 (99.999%, Takachiho) were used without further purification. Flow rates of WF_6 and SiH_4 were controlled by MFC (mass flow controller, Edward model 1605). Reactant gases were introduced through different inlet ports and mixed only on substrate. The total pressure in the reactor was maintained constant by using the adjustable outlet valve.

A 100-mm diameter P-(100) Si wafer was used, following pretreatment with 10% HF buffer solution for 1 min., then drying with nitrogen gas. Film surface and cross sections were examined by SEM (scanning electron microscope, Jeol JSM 840). Composition of the film was determined by AES (Auger electron spectroscope, Perkin-Elmer PHI 610). Crystal structure was deduced from XRD (X-ray diffraction, Jeol DX-GD-2) and SAED (selected area electron diffraction) patterns from TEM. Film

thickness and electrical resistivity were respectively measured by Dektak and four point probe. Film stress was measured by Stress measurement system (Tencor FLX 2320).

We deposited tungsten thin films using different gas conditions (WF$_6$ only or WF$_6$+SiH$_4$ mixture)as listed in *Table* 1. In WF$_6$+SiH$_4$ mixture run the mole ratio of WF$_6$/SiH$_4$ was set to 2. Annealing was carried out at 800℃ for 30 min. under vacuum condition.

RESULTS AND DISCUSSION

Under the cold-wall reactor condition, tungsten thin films were deposited via reduction of WF$_6$ by Si substrate or SiH$_4$ because the decomposition of WF$_6$ in gas phase was thermodynamically impossible below 2500K, $WF_{6(g)} \rightarrow WF_{5(g)} + F_{(g)}$: $\Delta H° =$ 135 kcal/mol[13]. In SiH$_4$ reduction of WF$_6$, we determined the crystal structure of tungsten thin film by using SAED and XRD techniques. SAED patterns are shown in *Fig* 2. where the first, second, third rings are calculated to correspond to W(110), W(200) and W(211) planes, respectively. *Fig.* 3(a) shows the X-ray diffraction spectrum showing a strong intensity at W(110), and weak intensities at W(200) and W(211) positions. The above SAED pattern and XRD spectrum indicate that the deposited film is mostly constituted by α-W which has bcc (body centered cubic) structure[14]. Even in the
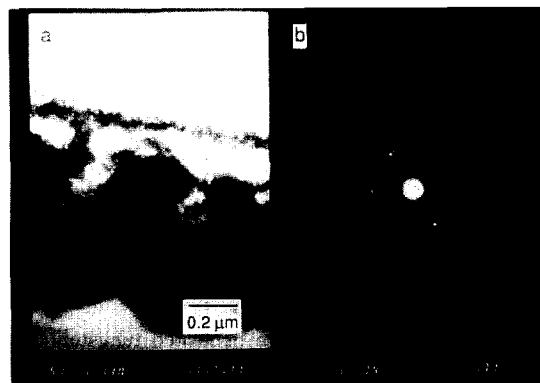

Fig. 2. (a) TEM micrograph of cross sectional area for the site of SAED analysis. (b) SAED pattern. The first, second, and third rings show W(110), W(200), and W(211) planes, respectively.

case of Si substrate reduction of WF$_6$ the XRD pattern (*Fig.* 3(c)) shows the W(110) peak. After 800℃ annealing, the crystal structure of the film was also investigated. The XRD spectrum is shown in *Fig.* 3(b), indicating no structural change upon annealing.

Table 2 lists the growth rate and roughness of tungsten films under different conditions. Surface roughness had been reported to be related to the
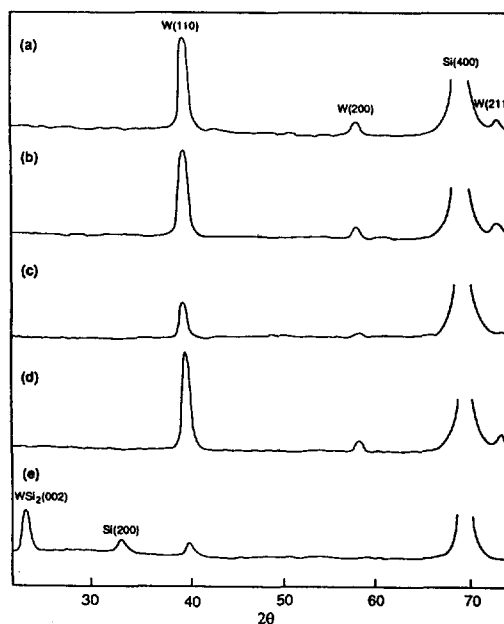

Fig. 3. X-ray diffraction spectra of tungsten film surface for (a) SiH$_4$ reduction of WF$_6$, cold-wall reaction, (b) SiH$_4$ reduction of WF$_6$, cold-wall reaction followed by annealing at 800℃, (c) Si reduction of WF$_6$ cold-wall reaction, (d) SiH$_4$ reduction of WF$_6$ hot-wall reaction, (e) SiH$_4$ reduction of WF$_6$, hot-wall reaction followed by annealing at 800℃.

Table 2. Growth rates and roughness under different conditions

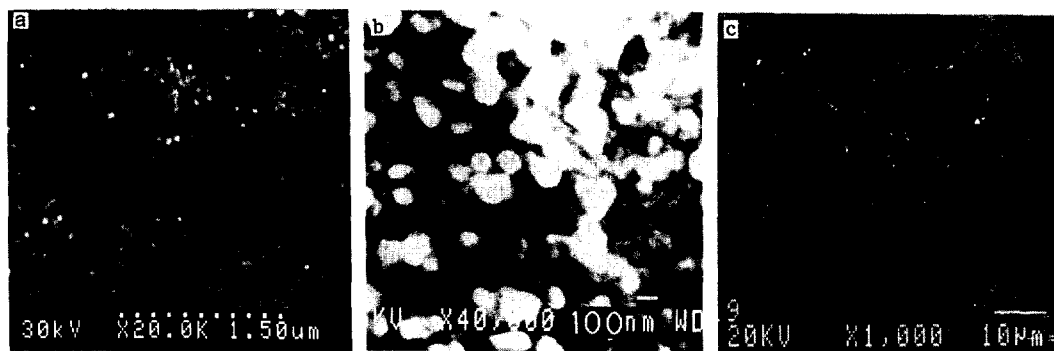| Reaction conditions		Growth rates (Å/min.)	Roughness (arb. unit)
Hot-wall		~3,000	600
Cold-wall	SiH$_4$ reduction	~300	30
	Si reduction	~5 (self-limited at ~300	10

Fig. 4. SEM micrographs of thin film surface for (a) Si reduction of WF_6, cold-wall reaction, (b) SiH_4 reduction of WF_6, cold-wall reaction, (c) SiH_4 reduction of WF_6, hot-wall reaction.

Table 3. Electrical resistivity under different conditions

Reaction conditions		ρ ($\mu\Omega$-cm)	
Cold-wall	as-deposited	Si reduction	14.5
		SiH_4 reduction	15
	800℃ annealed	Si reduction	13
		SiH_4 reduction	13
Hot-wall	as-deposited	132	
	800℃ annealed	115	

grain size[15]. Tungsten films by SiH_4 reduction had a rougher surface than those from Si substrate reduction, which may be caused by the increasement of the grain size as shown in *Fig.* 4(b). In the case of SiH_4 reduction the growth rate was ~300 Å/min. *Table* 3 shows the electrical resistivity values which are similar (about 15 $\mu\Omega$-cm) in any cold-wall case. These values are different from that of bulk tungsten the difference being partly due to matrix effect, which are caused by the disconnection of tungsten grains as shown in *Fig.* 4, and partly due to grain boundary scattering of charge carriers as Sivaram's report[16]. *Table* 3 also shows that the electrical resistivity value (~13 $\mu\Omega$-cm) of the annealed film is slightly lower than that (~15 $\mu\Omega$-cm) of the as-deposited one[17], which indicates the enhancement of the film property by annealing.

Fig. 4(a) shows the surface SEM micrograph in the case of Si substrate reduction of WF_6. Grains
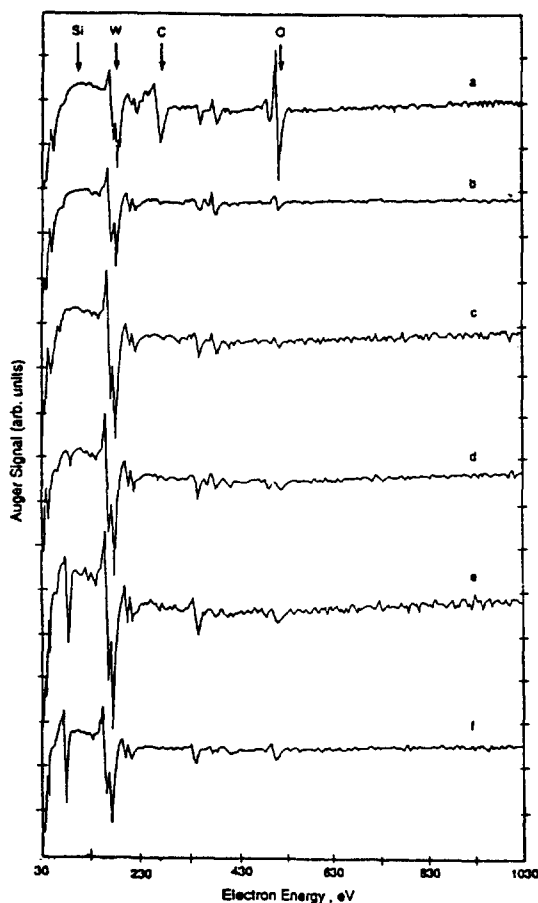

Fig. 5. Auger spectra of the deposited tungsten film from SiH_4 reduction of WF_6 and cold-wall reaction: (a) thin film surface, (b) after 1 min. sputtering, (c) after 10 min. sputtering, (d) after 40 min. sputtering, (e) after 50 min. sputtering, (f) after 60 min. sputtering.
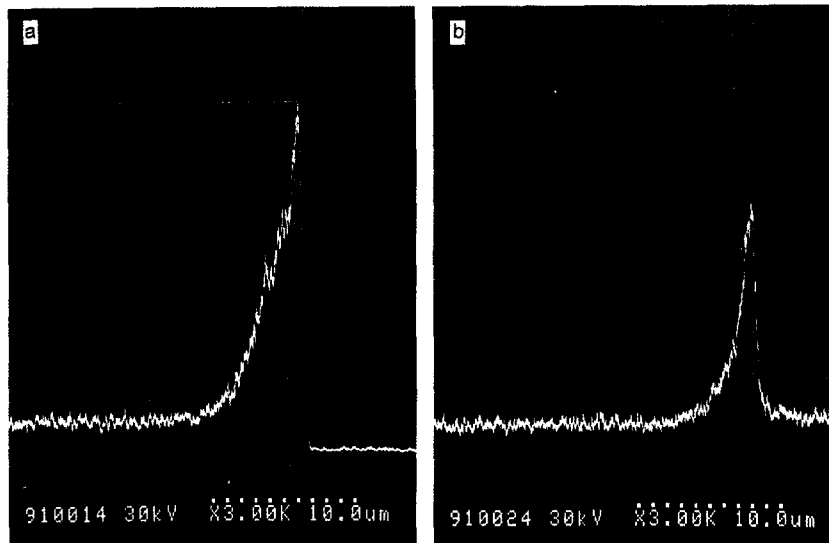
Fig. 6. Cross sectional X-ray mapping image of the tungsten film (a) as-deposited, (b) annealed at 800℃ . Dotted areas show the cross section of tungsten film.

and pores are seen on the film surface. It is believed that the appearance of porosity and grains is partly due to the coalescence of tungsten nuclei. In the case of SiH₄ reduction of WF₆ the surface SEM micrograph shows very compact grains developed on the film surface as shown in *Fig.* 4(b). *Fig.* 5 shows the AES depth profile of the film, which reveals that the density of the incorporated tungsten increase as the film grows in thickness. This result is also supported by the result of the cross sectional X-ray mapping of the film as shown in *Fig.* 6(a). The X-ray mapping was carried out by selecting only the tungsten L line to determine the relative tungsten concentration. We could also observe a more even distribution of tungsten concentration in the cross section of the annealed film than that of the as-dposited one (*Fig.* 6(a) and (b)) although the structure change did not occur by annealing. These results reveal that tungsten grains in the film were so tightly bound with each other, presumably as the island form, that could not be seperated by 800℃ annealing. Tungsten island, which has bcc structure, instead of tungsten atom may be shifted in the film by annealing. Therefore the number of chances for the reaction between W atom and Si atom, which is known to

be reacted at 600~700℃ [6], is few, and consequently the WSi₂ crystal structure can not be shown by 800℃ annealing.

Under the hot-wall reactor condition, tungsten thin film was deposited by SiH₄ reduction of WF₆. The film growth is estimated to be about 3000 Å/min. as shown in *Table* 1. This value is much larger than that of cold-wall case, by almost an order of magnitude.

Fig. 3(d) and (e) show the XRD spectra of the as-deposited and 800℃ annealed films in hot-wall reactor. The XRD spectrum for the annealed film shows a strong intensity at WSi₂(002) and weak intensities at Si(200), W(110) positions. This result reveals the occurrence of chemical reaction between W and Si to form WSi₂, which is known to have better compatibility than tungsten[11]. We expect that in the hot-wall reactor thin film tends to have voids and clusters, which are constituted by loosely bound W atoms, resulting from gas phase homogeneous reaction. The loosely bound W atoms are expected to move around rather freely during annealing and Si atoms also undergo significant bulk diffusion because of the void structure. Therefore W atoms may have a chance to meet Si atoms. Finally, they can form WSi₂.
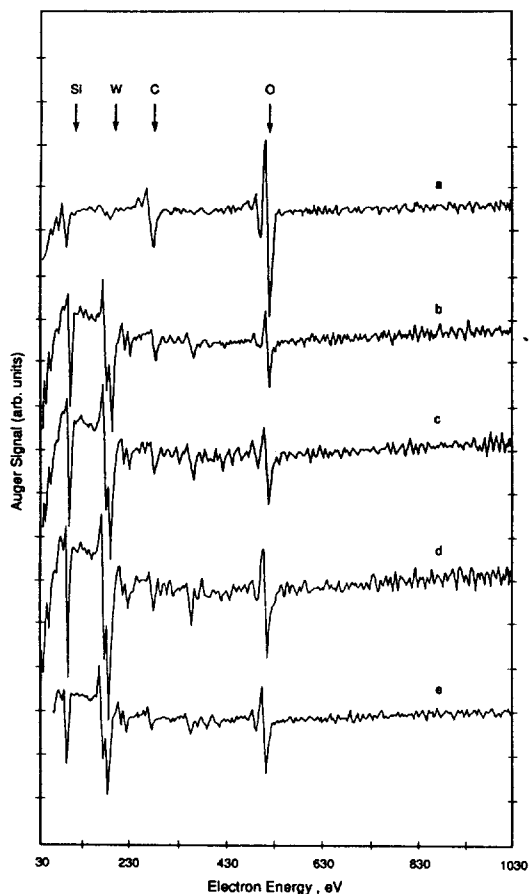
Fig. 7. Auger spectra of the deposited tungsten film from SiH₄ reduction of WF₆ and hot-wall reaction: (a) thin film surface, (b) after 5 min. sputtering, (c) after 10 min. sputtering, (d) after 20 min. sputtering, (e) after 30 min. sputtering.

The stress of as-deposited film and annealed film under cold-wall condition were measured as 17×10^9 dyne/cm² and 12.5×10^9 dyne/cm², respectively. However, under hot-wall condition, they were obtained as 31×10^9 dyne/cm² and 5×10^9 dyne/cm², respectively. Stress is a barometer of compatibility. Therefore, this results reveal that the compatibility is much enhanced by annealing under hot-wall condition because of the formation of WSi_2.

In order to analyze the composition of the hot-wall film, AES surveying was carried out. As shown in *Fig.* 5 and 7, the film from the hot-wall reaction has higher oxygen and silicon contents than that from cold-wall reaction. The film surface from hot-wall reaction (*Fig.* 4(c)) is found to be much rougher than that from cold-wall reaction as listed in *Table* 2. The electrical resistivity values of hot-wall films are also much higher than those of cold-wall films whether annealed or not (*Table* 3). Therefore we can conclude that hot-wall film has coarse structure and worse properties, which may be due to the contamination of silicon, oxygen or other impurity and surface roughness.

CONCLUSIONS

Tungsten thin film was deposited in LPCVD system using both cold-wall and hot-wall reactors. In both cases the structure of the deposited film can be understood to be a α-W which has a bcc structure. After 800°C annealing, the crystal structure of the film in cold-wall reactor would not be changed, however, that of hot-wall reactor changed into WSi_2. It turned out that the film properties of cold-wall reactor is better than those of hot-wall reactor.

ACKNOWLEDGEMENTS

REFERENCES

1. Broadbent, E. K.; Stacy, W. T. *Sold State Technol.* **1985,** *28*, 51.
2. Black, J. *IEEE Trans. Electron Devices* **1969,** *ED-00*, 338.
3. Vossen, J.; Schnable, G.; Kern, W. *J. Vac. Sci. Technol.* **1972,** *9*, 515.
4. Kaanta, C.; Cote, W.; Cronin, J.; Holland, K.; Lee, P.; Wright, T. *IEDM Tech. Dig.* **1987,** *12*, 209.
5. Crowder, B. L. Zirinsky, S. *IEEE Trans. Electron Devices* **1979,** *ED-26*, 369.
6. Sze, S. M. *VLSI Technology;* McGraw-Hill: 1988; p 383.
7. Sherman, A. *Chemical Vapor Deposition for Microelectronic;* Noyes Publications: 1987; p 106.

8. Brors, D. L.; Fair, J. A.; Monnig, K. A.; Sarawat, K. C. *Solid-State Technol.* **1983**, *26*, 283.

9. Broadbent, E. K.; Ramiller, C. L. *J. Electrochem. Soc.* **1984**, *131*, 1427.

10. Green, M. L.; Levy, R. A. *J. Electrochem. Soc.* **1985**, *132*, 1243.

11. Ohba, T.; Inoue, S.; Maeda, *Proc. IEEE IEDM Tech. Dig.* **1987**, 213.

12. Kotani, H.; Tsutsumi, T.; Komori, J.; Nugao, S. *IEEE IEDM Tech. Dig.* **1987**, 217.

13. Stull, D. R. *et al., JANAF Thermochemical Tables,* 2nd Ed.; 1971; p 37.

14. Busta, H. H.; Tang, C. H. *J. Electrochem. Soc.* **1986**, *133*, 1195.

15. Kamins, T. I.; Bradbury, D. R.; Cass, T. R.; Laderman, S. S.; Reid, G. A. *J. Electrochem. Soc.* **1986**, *133*, 2555.

16. Sivaram, S.; Tracy, B.; Waston, L. *Proceedings of the 10th International Conference on CVD* **1987**, *87/88*, 614.

17. Shioya, Y.; Itoh, T.; Kobayashi, I.; Maeda, M. *J. Electrochem. Soc.* **1986**, *133*, 1475.